A quasi steady state approach to race car lap simulation in order to understand the effects of racing line and centre of gravity location

D L Brayshaw and **M F Harrison***
School of Engineering, Cranfield University, Cranfield, UK

The manuscript was received on 13 June 2003 and was accepted after revision for publication on 13 January 2005.

DOI: 10.1243/095440705X11211

Abstract: Using an established seven-degree-of-freedom (7DOF) model of an open wheel race car, a new quasi steady state lap simulation method is described. The method is based on optimal control techniques. It produces a GG speed diagram as an interim result, and is shown to have a low computational expenditure when compared with the current transient optimal control method. This paper shows a validation step, reports a case study using the new method, and compares the result with a transient optimal control method. The sensitivity of the optimal line for simulation studies is discussed in terms of a centre of gravity location change. Both simulation methods show improvements in lap time owing to a 6 per cent centre of gravity set-up change. The difference in optimal lines caused by a 6 per cent CG change rearward is shown to be so small that a driver is unlikely to find the information useful. In light of this observation, the computational effort required to generate a new optimal line for each set-up change may be misspent.

Keywords: vehicle, simulation, optimal, quasi, steady state, transient, racing line, path

1 INTRODUCTION

From the point of view of designers and engineers, lap time simulation needs to perform three functions: it needs accurately to model the dynamic behaviour of the vehicle, it needs accurately to predict lap times, and it needs to produce lap simulation results rapidly, to allow many different vehicle set-up and configuration changes to be examined for a particular circuit.

Lap simulation methods have been produced by a variety of different researchers, notwithstanding the programs generated by race teams that are not published in the interests of maintaining a competitive advantage over other teams. Lap simulations can be considered to fall into three main types: steady state, quasi steady state, and transient (sometimes optimal control based). Steady state models will not be discussed in this paper because of their oversimplicity and lack of ability accurately to represent the vehicle in lap time simulations, as seen in reference [**1**].

1.1 Quasi steady state (QSS) models

The use of quasi steady state models has been widespread across the automotive industry [**1–5**]. A car that accelerates, brakes, and corners in a smooth fashion can be modelled approximately by joining together a series of static equilibrium or steady state manoeuvres. The circuit is broken into segments, and the local curvature is calculated for each segment. The static equilibrium or steady state behaviours can be generated for each segment from either a dynamic or a steady state vehicle model. The overall process, regardless of the method of determining the vehicle states, is the quasi steady state approach to vehicle–circuit simulation.

Of the quasi steady state lap time simulation programs reported in the literature, it appears that there are two methods of producing the static equilibrium or steady state behaviours for a lap simulation of a

* *Corresponding author: School of Engineering, Optical and Automotive Engineering Department, Cranfield University, Cranfield, Bedfordshire MK43 0AL, UK. email: m.harrison@cranfield.ac.uk*

circuit. Siegler *et al.* [**1**] generate the points interactively, while Candelpergher *et al.* [**2**] and Blasco-Figueroa [**3**] access an independently generated GG speed diagram. These diagrams are discussed in references [**6**] and [**7**].

The research presented in reference [**1**] is a comparison of steady state, quasi steady state, and transient programs for cornering manoeuvres using a three-degree-of-freedom (3DOF) model. To find the maximum lateral acceleration that the car is able to maintain through a corner, the quasi steady state program iterates using a Newton–Raphson method, altering the steer angle until it finds the peak lateral acceleration for the given cornering radius. The quasi steady state approach was found to be a good approximation to the transient model in the cornering manoeuvres.

A quasi steady state program that operates on a GG speed diagram has been produced by Blasco-Figueroa [**3**]. The program requires the trajectory to be defined in terms of curvature and distance travelled. The GG speed diagram is generated from a seven-degree-of-freedom (7DOF) model [**8**]. The program identifies peaks in the curvature data as an apex of a corner. At each apex, the program calculates the vehicle speed profile from the acceleration data up to the next apex. Similarly, the program then calculates the vehicle speed profile from deceleration data from the second apex back to the first apex. Where accelerating and braking vehicle speeds in between two apexes reach the same value, the vehicle stops accelerating and starts braking. The program achieves this by switching at this point from the vehicle speed profile from the acceleration data to the vehicle speed profile from the braking data. The program runs very quickly (a simulation of the Barcelona Grand Prix circuit on a 266 MHz Intel processor takes just under 60 s) and robustly.

The program outlined in reference [**2**] also operates from a GG speed diagram, but the vehicle model used is not described. The paper emphasizes that the computational speed of their simulations was improved by estimating the GG speed diagram before simulating a lap. Like Siegler *et al.* [**1**], Candelpergher *et al.* [**2**] also use iterative methods to determine the accelerating and braking zones for the vehicle model. The program iterates to make the speed at the end of the acceleration zone meet the braking zone, if the car is not able to reach full speed before reaching the braking point for the next corner. Iterative processes can be computationally expensive, and there is no guarantee they will converge. The approach of Blasco-Figueroa [**3**] working backwards from the new apex to the old one for braking, and then working forwards from the old apex to the new one and identifying the crossover point, appears to be simpler and more robust.

1.2 Transient-optimal (TO) control

Transient methods of lap simulation involve the numerical integration of the vehicle equations of motion with respect to time. This is different to the QSS methods which form a simulation history from the succession of quasi steady state manoeuvres used to follow a prescribed trajectory. The simulation time found from a QSS method is a consequential variable evaluated from the distance travelled along the trajectory and the vehicle speed, whereas time is an independent variable in a transient simulation.

There are many computer programs such as ADAMS [**9**] that use transient simulation to show the time varying response of a vehicle to specific manoeuvres, but, for the purpose of this paper, only a subset of the transient method research field, transient-optimal control, will be discussed. This is because this area of transient-optimal control simulation is focused on controlling the vehicle models to produce the fastest lap time possible, creating the desired situation where the vehicle is controlled to its performance capability limit.

An early 3DOF transient optimal control model was produced by Fujioka and Kimura [**10**]. This model was used to optimize simple cornering manoeuvres with different driving and steering configurations. A simple lap time optimization using a linear 3DOF vehicle model was produced by La Joie [**11**].

The next significant improvement was a vehicle model with three DOF, an engine torque curve, a nonlinear tyre model, and a steady state approximation of the aerodynamic forces and load transfer [**12**]. As in reference [**10**], the model was employed for single manoeuvres, but additionally the vehicle path was not prescribed and was only limited by constraints on the vehicle states.

A direct shooting method for employing optimal control for vehicle simulation has been investigated by Allen [**13**]. Direct shooting, or direct searching, methods rely only on evaluation of the problem $(f(x))$ at a sequence of points $x_1, x_2, \ldots$ and comparing values in order to reach the optimal point x^* [**14**]. This method provides a discrete approximation to the continuous problem and allows the optimal control problem to be formulated as a nonlinear programming problem and then solved using mathematical programming techniques. This method was applied to a vehicle model similar to that in reference [**12**].

The research conducted by Casanova [**8**] has also focused on more efficient optimal control algorithms. His research expands on previous models, by extending the vehicle model to include seven DOF, an engine map specified by engine speed as well as throttle position, and a combined slip form of the Pacejka magic formula tyre model [**15**]. His research extends to a complete lap optimization of two Grand Prix circuits.

At present, Casanova's work [**8**] appears to be the state of the art. No other work has been published, to the author's knowledge, that optimizes a transient non-linear race car model over a complete lap of a circuit. The vehicle model has been used to conduct mass [**16**], centre of gravity [**17**], and vehicle yaw inertia sensitivity studies [**18**], which have produced results that are in agreement with results obtained from an F1 car. Unfortunately, the computational time for solution is very long (it can be more than 24 h) and the success of the program is reliant on the user's knowledge of the driver–vehicle relationship with respect to cornering and straight-line negotiations to improve significantly the computational time and produce a solution. Additionally, judicious choice of the circuit segmentation is necessary for the method to work reliably.

At Cranfield University, lap time simulation has been progressing for many years under the direction of R. S. Sharp, and has more recently been applied to open wheel race cars. Griffiths [**19**] produced a basic lap simulation method for an open wheel race car. Minimum time optimal control for cornering has also been investigated [**13**]. More recently, full lap time optimization has been a topic of research [**8**]. GG speed diagram based research began being applied to race cars by Blasco-Figueroa [**3**] using diagrams generated from an optimal control-based method [**8**], and more recently a GG diagram has been produced from a series of dynamic simulations of a simple vehicle model by Murdoch [**20**].

1.3 New research

The current research aim is to find methods of improving the speed of lap time simulation while maintaining the accuracy achieved by Casanova [**8**]. At present, one hypothesis is that the computational time can be reduced by supplying the racing line rather than computing it as part of the lap time optimization, without losing accuracy in the evaluation of the vehicle states. Of course, the benefits of finding the optimal line are lost.

A GG speed diagram generation program has been developed for the same 7DOF vehicle model as used by Casanova [**8**]. In conjunction with a new QSS simulation program based on the method described by Blasco-Figueroa [**3**], the GG speed diagrams are used to produce lap times and vehicle state and control histories for open wheel race cars at Grand Prix circuits. The vehicle configuration discussed here is based on a particular open wheel race car.

2 QSS METHOD

The GG speed diagram is generated from the results of a series of dynamic equilibrium problems that are solved by the constrained non-linear optimization routine *fmincon* implemented in MATLAB [**21**]. The optimizer is supplied with an initial guess of the vehicle limit states. These states are a mixture of system inputs and unknown quantities, and the unknowns vary depending on the application. Equation (1) shows the possible components of the optimization vector, $\boldsymbol{P}$

$$\boldsymbol{P} = [\dot{x}, \ddot{x}, \dot{y}, \dot{\varphi}, \dot{\theta}_{\mathrm{LF}}, \dot{\theta}_{\mathrm{RF}}, \dot{\theta}_{\mathrm{LR}}, \dot{\theta}_{\mathrm{RR}}, \delta, T_{\mathrm{p}}]^{\mathrm{T}} \tag{1}$$

Initially, the GG diagram program finds the maximum possible speed of the vehicle. It is clear that the vehicle will travel in a straight line to achieve this. This assumption allows us to reduce the optimization vector, $\boldsymbol{P}$, to

$$\boldsymbol{P} = [\dot{x}, \dot{\theta}_{\mathrm{F}}, \dot{\theta}_{\mathrm{R}}, T_{\mathrm{p}}]^{\mathrm{T}} \tag{2}$$

where $\dot{\theta}_{\mathrm{F}}$ and $\dot{\theta}_{\mathrm{R}}$ are the front and rear wheel angular speeds which are assumed to be identical for each side of the vehicle.

The objective function is simply

$$f = -\dot{x} \tag{3}$$

The solver is a minimizer, and therefore a negative sign is required in equation (3). Once the maximum possible speed of the vehicle is known, the next task is to evaluate the maximum positive and negative longitudinal accelerations possible with the vehicle operating at increments of the maximum speed in order to take account of aerodynamic forces that change with vehicle speed. The optimization vector, $\boldsymbol{P}$, and the objective function, f, now become

$$\boldsymbol{P} = [\ddot{x}, \dot{\theta}_{\mathrm{F}}, \dot{\theta}_{\mathrm{R}}, T_{\mathrm{p}}]^{\mathrm{T}} \tag{4}$$

$$f = \pm\ddot{x} \tag{5}$$

Once the longitudinal acceleration and deceleration capabilities of the vehicle at various speeds have been calculated, the task of filling the remainder of the GG speed diagram can be split into a set of optimizations at increments of the maximum longitudinal acceleration/deceleration for each speed increment. This is the most difficult task, because the number of variables in the optimization vector increases significantly

$$\boldsymbol{P} = [\dot{y}, \dot{\varphi}, \dot{\theta}_{\mathrm{LF}}, \dot{\theta}_{\mathrm{RF}}, \dot{\theta}_{\mathrm{LR}}, \dot{\theta}_{\mathrm{RR}}, \delta, T_{\mathrm{p}}]^{\mathrm{T}} \tag{6}$$

The objective function becomes the maximum steady state lateral acceleration that the vehicle is capable of

$$f = -\dot{x}\dot{\varphi} \tag{7}$$

At all times the optimizer is constrained to find the solution to the equations of motion that gives the static equilibrium or steady state condition required. The constraint matrix **G** is given as follows

$$\mathbf{G} = \begin{bmatrix} \ddot{y} & = & 0 \\ \ddot{x} & = & -\text{target longitudinal acceleration} \\ \ddot{\varphi} & = & 0 \\ \ddot{\theta}_{\mathrm{LF}} & = & f_1(\ddot{x}) \\ \ddot{\theta}_{\mathrm{RF}} & = & f_2(\ddot{x}) \\ \ddot{\theta}_{\mathrm{LR}} & = & f_3(\ddot{x}) \\ \ddot{\theta}_{\mathrm{RR}} & = & f_4(\ddot{x}) \\ \text{Engine torque} & \leqslant & \text{Maximum engine torque} \end{bmatrix}$$

Parameters $\ddot{y}$ and $\ddot{\varphi}$ are the acceleration through the y axis and the yaw acceleration, which must both be zero. These are conditions of steady state cornering. Functions $f_i(\ddot{x})$ describe the wheel accelerations in terms of longitudinal acceleration of the vehicle. The engine torque is also included as a constraint because of the tendency of the optimizer to explore throttle positions beyond fully open. The fully open throttle is assigned the value of 1, and full braking is assigned the value of -1. The engine map is stored as a two-dimensional look-up table with a maximum throttle position of 1, so there are times when this constraint is required to keep the optimizer within the limits of the problem.

The GG speed diagram generation process is shown diagrammatically in Fig. 1. When these optimizations are solved for both tractive and braking conditions, all the necessary information to produce a GG speed diagram is available.

The 7DOF vehicle model is quite comprehensive, and as a result a large quantity of information is available for analysis. Table 1 shows the primary variables that are produced by the optimization program either as an optimal set of the vector $\boldsymbol{P}$ or as system inputs to the model. It is possible to

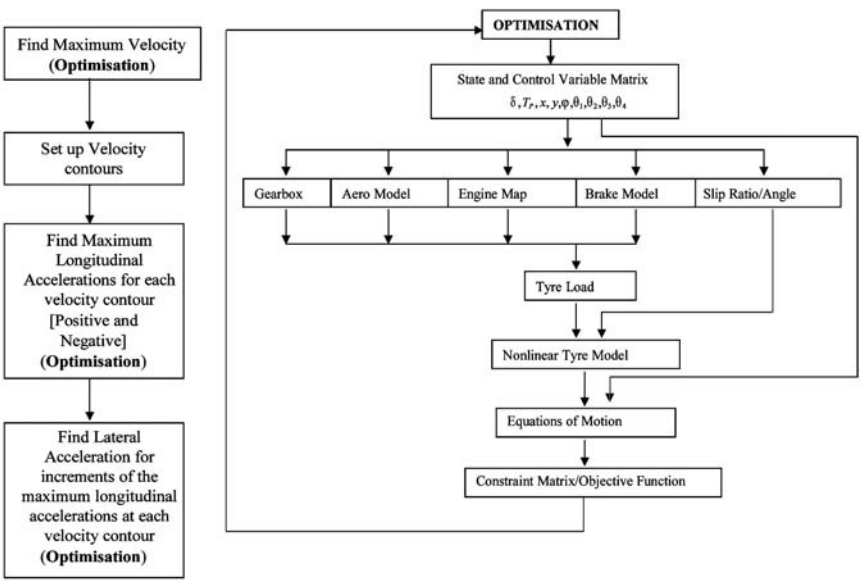

Fig. 1 Optimization routine

Table 1 GG speed optimization output

Program output	Variables
Primary variables (state and control variables)	Throttle position, steer angle, individual wheel speeds, yaw rate, lateral velocity, and lateral and longitudinal acceleration
Consequential variables	Individual longitudinal and lateral tyre forces, aerodynamic lift and drag forces, brake and engine torques, slip angle and slip ratio, and individual tyre loads

produce, in conjunction with a lap simulation program, data histories for an entire lap for all the vehicle states and forces listed.

2.1 GG speed diagram

The base vehicle set-up is the original specification for a particular open wheel race car at the Barcelona circuit [**8**]. This particular vehicle set-up and circuit were chosen because they had been validated by a Formula One team with telemetry data. The vehicle model, in this condition, is used to produce the GG speed diagram to be used as the vehicle performance envelope for a lap simulation program. The result is shown in Fig. 2.

The GG speed diagram shows that the vehicle performance envelope is quite smooth, but the longitudinal acceleration is sensitive to small changes in lateral acceleration near the maximum lateral acceleration values. The optimizer has been effective in maximizing the lateral acceleration for a given vehicle speed and longitudinal acceleration in most cases, showing the trends expected for this type of race car [**7**].

2.2 Description of the current QSS simulation

2.2.1 Assumptions

To find a sensible balance between computational speed and accuracy of simulation, it is important to consider the assumptions that have been made in the simulation method, and what influence they will have on the results obtained. The term 'quasi steady state', as it is applied here, means that the vehicle can be modelled traversing a racetrack, split into segments, as a set of dynamic equilibrium manoeuvres. The condition that must hold for the quasi steady state assumption to be valid is that the changes in vehicle states occur slowly between adjacent segments. This can be achieved by making the segment spacing small.

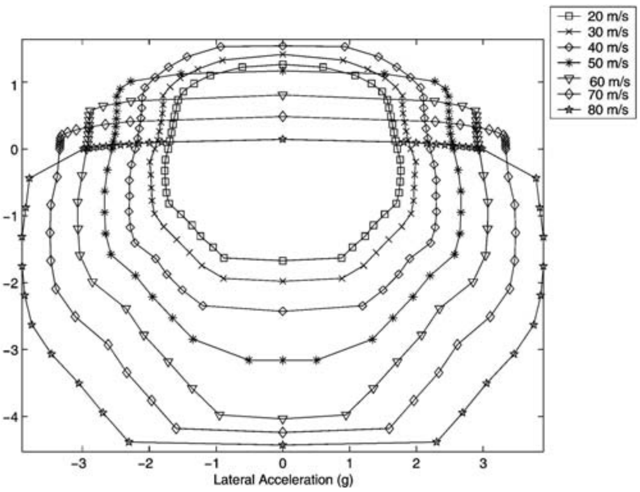

Fig. 2 GG speed diagram – base set-up

The racing line is described in terms of curvature. This can be done in three ways:

1. It can be produced from a set of telemetry-based lateral acceleration and vehicle speed data.
2. A sensible racing line can be drawn on a facsimile of the track profile and the curvature information calculated using basic geometry.
3. It can be produced from a transient optimal control simulation.

The transient effects of changing the state of the vehicle are neglected in the simulation. A step change in steer angle and throttle position in the simulation from one segment to the next results in the vehicle assuming its new state instantly. Even with fine segmentation of the track description, this is an approximation. When the car is braking and accelerating, the car is assumed to respond instantly to the longitudinal forces provided by the tyres. This is an approximation of the real situation.

As discretized segments are used to represent the race track, there is constant acceleration between segments. Therefore, the QSS simulation will produce smoother acceleration profiles than those generated by a real race car.

2.2.2 Description of the current lap simulation program

The basis of the lap simulation program is a calculated GG speed diagram. The lap simulation program interpolates between the points on the GG speed diagram to find the vehicle acceleration that is possible given the track description.

The program identifies peaks in the curvature data as an apex of a corner. Between a pair of apexes, the program calculates the maximum acceleration possible from apex i up to apex $i+1$ (Fig. 3). This procedure is carried out for all apex pairs encountered over the entire lap.

The program then calculates the maximum braking deceleration possible between all apex pairs. Given the maximum possible accelerations and decelerations between apex pairs, acceleration and deceleration speed profiles can be calculated.

The crossover point is where the accelerating and braking speeds between two apexes reach the same value (Fig. 3). At this point, the program switches

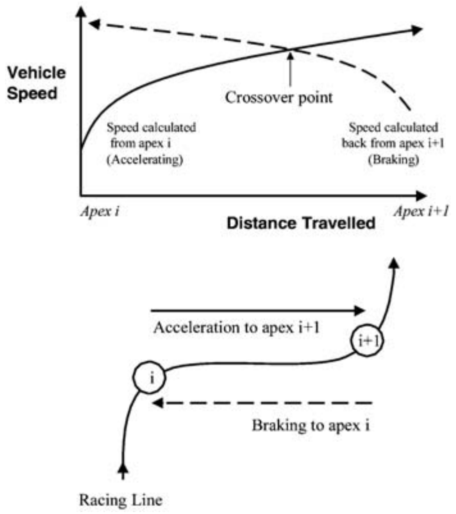

Fig. 3 QSS simulation principle

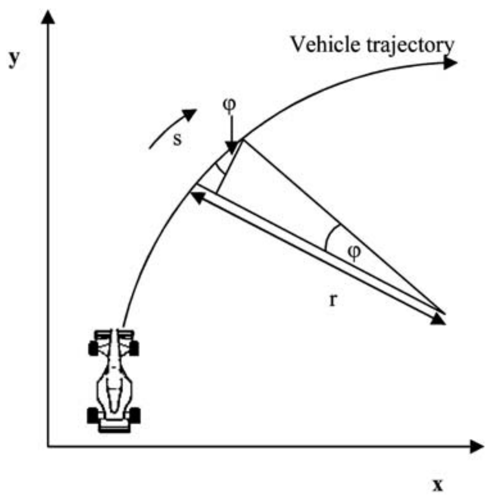

Fig. 4 Trajectory coordinate relationships

from the acceleration data to the braking data, providing a realistic transition point from acceleration to braking.

2.2.3 *Effects of curvature*

The main difficulty with this lap simulation method is that the results are very sensitive to small changes in the track curvature information. Initial trials showed that a smooth trajectory dataset was vital for the program to produce realistic results. Curvature information can be obtained from telemetry, or from a Cartesian coordinate description of a racing line that has been drawn from experience, or from results of a transient optimal control lap simulation method.

Telemetry results can readily produce a racing line in terms of curvature. If it is assumed that the vehicle is cornering in steady state, the track curvature can be calculated from the time histories of the lateral acceleration and vehicle speed data using the relationship

$$r = \frac{\dot{x}^2}{a_y} \tag{8}$$

Telemetry noise from vehicle vibrations, measurement errors, and calibration errors make it difficult to find the actual curvature from the data. These errors are manifested as both high-frequency noise and offset in the recorded data. Therefore, it is important to exercise caution when evaluating curvature from telemetry information in this manner.

To find track curvature from a set of Cartesian points (as might be obtained from a transient optimal simulation), the first step is to calculate the yaw angle, φ, of the car on the given trajectory. The geometry of the trajectory causes the following relationships

$$\varphi = \arctan \frac{\mathrm{d}y}{\mathrm{d}x} \tag{9}$$

Differentiating φ with respect to distance travelled

$$\frac{\mathrm{d}\varphi}{\mathrm{d}s} = \frac{1}{r} \tag{10}$$

To produce a curvature versus distance representation, φ is evaluated for each set of Cartesian coordinates, and the distance travelled between the coordinates is approximated by a straight line.

In the QSS simulation method described here, a second-order polynomial is fitted to the relationship between φ and s. Good results are obtained with a number of points that represent approximately half the length of the tightest corner on the circuit when the spacing between points is 2 m. Taking the analytical derivative of the polynomial, equation (10) can be evaluated, producing the curvature information required.

Track curvature calculated from a set of Cartesian points includes errors from the polynomial fitting procedure and the approximation of s, but this can be controlled by sensible discretization of the lateral and longitudinal distance points. Therefore, this method was preferred to one based on telemetry data and was used to produce the results here.

3 RESULTS

3.1 Validation using the published vehicle model

For initial validation of the GG speed diagram calculation and the lap simulation method, a comparison of distance-based acceleration histories with the validated and published results of a TO method (Fig. 5) [**8**] are shown in Fig. 6. These are for a simulation of the Grand Prix Barcelona circuit, Catalunya. The racing line used in both methods is shown in Cartesian form in Fig. 7.

The agreement in the acceleration calculations shown in Fig. 6 is generally very good. The main differences can be seen in the longitudinal accelerations when the vehicle is experiencing high lateral acceleration. This can be accounted for by the shape of the GG speed diagram at high lateral accelerations where the gradient with respect to longitudinal acceleration is very steep. The QSS results oscillate around the value produced by the TO method [**8**].

There also appears to be a constant delay in some corner entry and exit points when comparing the results of the two methods. This is attributed to the different braking and acceleration crossover points used by the two methods, especially in corners 9 to 11.

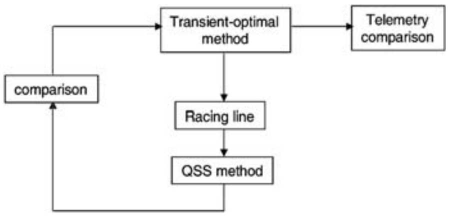

Fig. 5 QSS method validation

The lap time difference between the two methods is 2.19 s (Table 2), which is a significant difference. This appears to be a function of the different braking/accelerating crossover points used by the two methods, and is not easy to remedy using the current simulation method. However, the close agreement of the acceleration magnitudes during cornering suggests that the vehicle is traversing the path on, or very close to, the limit capability of the vehicle. Therefore, for comparative analysis of vehicle set-up and configuration changes for a given trajectory, the method will be suitable for determining whether the vehicle is comparatively faster or slower on account of those changes. Since the accurate modelling of tyres and friction coefficients is so difficult to achieve, lap time simulation programs are generally not employed for the purposes of determining the expected lap time of an actual vehicle. The purposes of lap time evaluation are generally for determining whether changes to that vehicle have made the vehicle faster or slower around the circuit owing to set-up changes to the vehicle [**2**].

Table 2 Lap time at the Barcelona Grand Prix circuit for the QSS and TO methods

Lap time (s), QSS	Lap time (s), TO
82.904	80.714
Difference	2.19

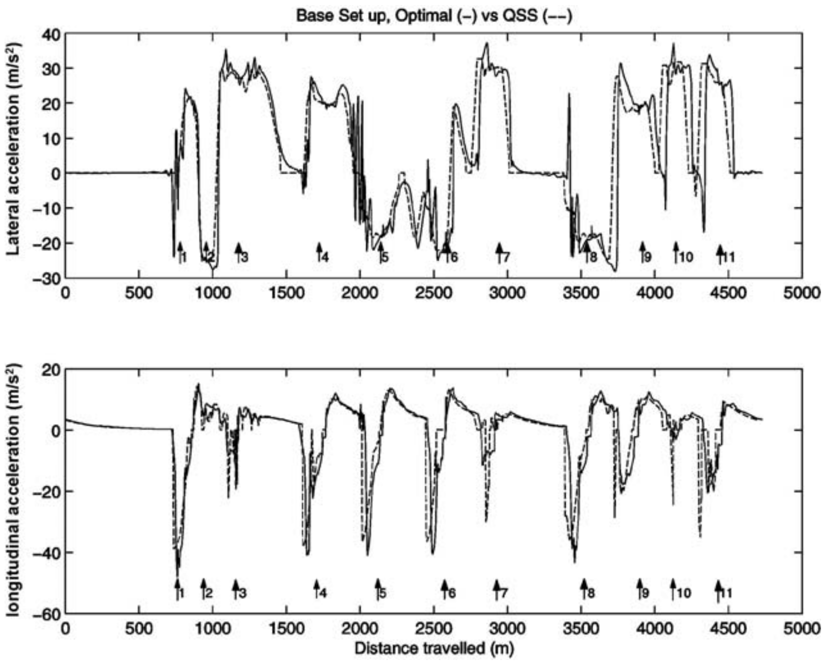

Fig. 6 Comparison of QSS and TO methods [arrows show corner locations (see Fig. 7)]. The TO method is from reference [**8**]

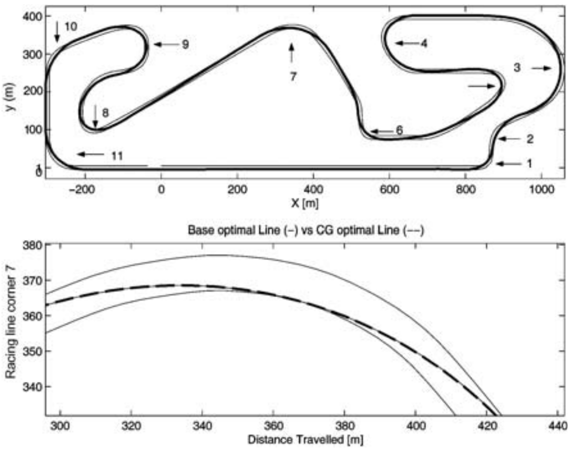

Fig. 7 Racing line, Barcelona Grand Prix circuit

While the results produced by the current QSS method are very similar to those produced by Casanova [**8**], more simplifying assumptions have been made. The driver for this was the saving in computational time required to produce the result. Over an average of 24 individual optimization runs for the Barcelona circuit, the processing time was 39.8 h on a Sun workstation for the method in reference [**8**]. The QSS method took an average of 10 complete runs with different vehicle set-ups, only 16 min on an Intel 1000 MHz PC. The processing time can vary on account of the iterative nature of the optimization process when the vehicle set-up is changed. The simplifying assumptions of the QSS method have allowed a dramatic improvement in computational time, allowing more vehicle set-up and vehicle design scenarios to be performed by the analyst, without great changes in the results obtained with respect to the TO method.

4 CASE STUDY – THE OPTIMAL LINE

The optimal line is important because it helps identify the fastest possible lap time that can be achieved by the vehicle in its current set-up condition for a particular circuit. It is theoretically possible to determine the optimal line by experiment. Extensive testing of the vehicle at the circuit with a world-class driver who spends hours trying to improve his/her laptime would approach the optimal line eventually if sufficient time was available and the driver's skill was sufficient to control the vehicle on the limit of the performance envelope of the car. In general, the huge cost of testing and the inherent variability in driver performance negate this as a genuine method for determining the optimal line. Also, finding ways of capturing actual racing lines has never been easy, and, even with the aid of global positioning systems (GPSs), the task is both expensive and rather difficult [**22**].

Computer simulation offers another possibility. Optimal control techniques have begun to be applied to this problem with reasonable success. This method has been employed from negotiating simple manoeuvres [**4**, **12**, **23**] to the full circuit racing line [**8**]. These methods remove the variability of driver skill but, to make the problem solvable in a reasonable time, require that simplified mathematical models of the vehicle be used. Results from computer simulations will be examined and discussed in the following sections.

4.1 Accuracy of optimal racing line calculation

Optimization is an iterative process. An objective function is minimized or maximized subject to a set of constraints being met. Termination criteria are set as part of the computer program. The termination criteria normally define the worst-case constraint violation that is acceptable at the solution and also the precision required of the independent variables in order to call the solution optimal [**21**]. Consequently, the simulation engineer must decide the level of accuracy and precision that is required. This will generally be a trade-off based on achieving an acceptable computational time and accuracy at the solution.

It is first prudent to determine the accuracy of the optimal solution given the available information. Student's t-statistic will be used because the true standard deviation about the optimal solution is not known. To determine whether an optimal solution is likely to be a global or local minimum (or maximum), the TO program is started from different values of the optimization vector variables. The results are replicate solutions. If the optimizer converges on the same solution from many different starting points, then this adds weight to the supposition that the solution found is global.

As mentioned in section 3.1, the computational time for an existing method for an entire lap is quite long. Of the results obtained in reference [**8**], only four replicates were able to be produced in the time available for each vehicle parameter that was studied.

Figure 8 shows the differences in the three replicate optimal racing lines with respect to the candidate global line that produced the fastest lap time. The dotted line represents the 95 per cent confidence interval for the differences in the racing lines about the fastest line, which was found to be ± 0.5 m. This is relatively small in the context of a circuit that is nominally 10 m wide.

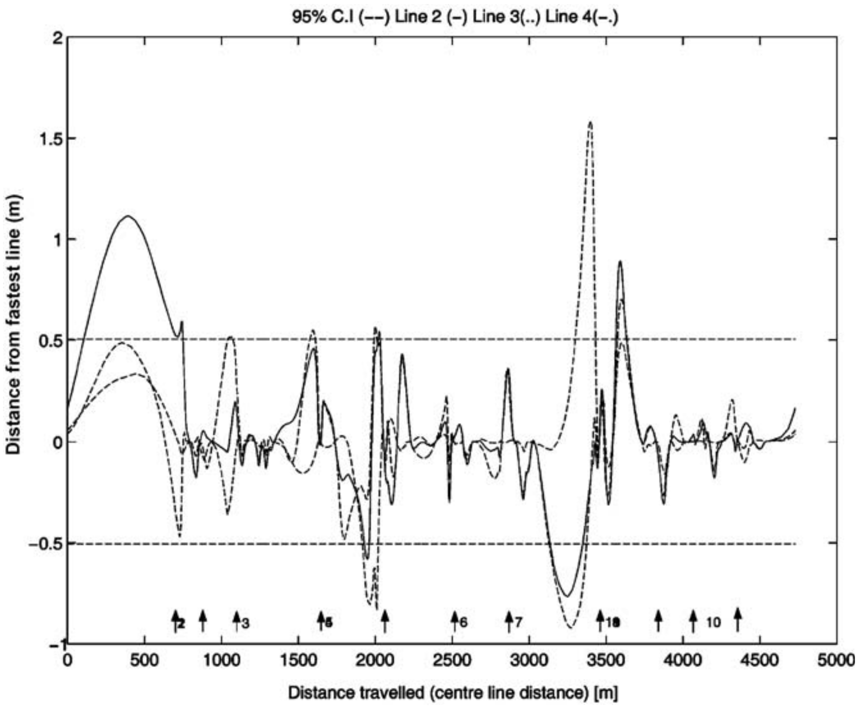

Fig. 8 Difference in optimal racing lines calculated by the TO method

4.2 Vehicle parameter changes

Now that the size of the optimal path zone can be described (± 0.5 m), it is possible to apply the optimal line results to the QSS simulation method and investigate the effects of changing vehicle parameters.

The location of the centre of gravity (CG) is a sensitive and therefore dominant design variable in automotive design [**24**]. The general trend, notwithstanding the non-linear effects of vertical load on the tyre forces, is that a move of the CG rearward will promote oversteer [**25**]. In effect, the car will be harder to control on the limit, but could be potentially faster round the circuit. A rearward weight bias can improve traction for a rear wheel drive vehicle. Although the effect of the CG position has been investigated elsewhere [**17**], the use of the current QSS method on two alternative racing lines has identified further behavioural attributes of the racing car that are worthy of discussion.

4.2.1 GG speed diagram

A modest change of 6 per cent towards the rear in the location of the CG has been introduced as a change to the base vehicle set-up. The GG speed diagram is recalculated and the result is shown in Fig. 9.

The differences between the new GG speed diagram and the base car (Fig. 9) can be summarized as follows.

1. Lateral acceleration generation capability has improved for the tractive part of the diagram.
2. Lateral acceleration generation capability has decreased for the braking part of the diagram.

The lack of smoothness in the velocity contours in Fig. 9 of the 6 per cent rearward CG result, when compared with the base result, is indicative of the difficulty the optimization routine had in trying to solve the equations of motion to produce the GG speed diagram. It is obvious that the model performance is not a smooth function of the state variables. It is often difficult to find the optimum. Clearly, the method struggles with this task, and a similar difficulty was found by Casanova *et al.* [**17**] with their TO method. The natural conclusion is that, under this new set-up, the model is extremely sensitive to small changes in the control inputs. This is mainly evident in the braking part of the diagram. Instability under braking does not inspire any driver to brake late into corners, and it is possible to imagine that this set-up change would not be a desirable one to increase driver confidence in the vehicle.

4.2.2 New optimal line

When vehicle parameters are changed, it is reasonable to assume that there will now be a new optimal line to extract the fastest possible lap time from the vehicle. The results of reference [**17**] indicate that this was indeed the case.

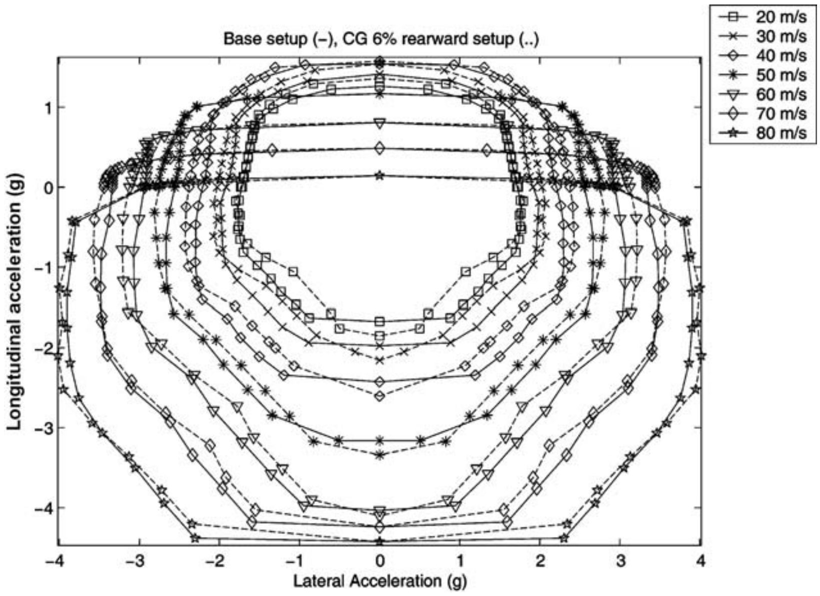

Fig. 9 GG speed diagram – base set-up versus CG set-up

For clarity, the optimal line found for the base set-up will be referred to as the 'base optimal' line, and the optimal line found for the set-up shown in Fig. 9 will be referred to as the 'CG optimal' line. The CG set-up will be referred to as the 'CG vehicle' and the base set-up will be called the 'base vehicle'.

When plotted in terms of Cartesian coordinates as in Fig. 7, the differences between the two optimal lines are very hard to see. Instead, the distance from the centre-line of the track has been calculated at each time step for both optimal lines, and the difference between the two is shown in Fig. 10.

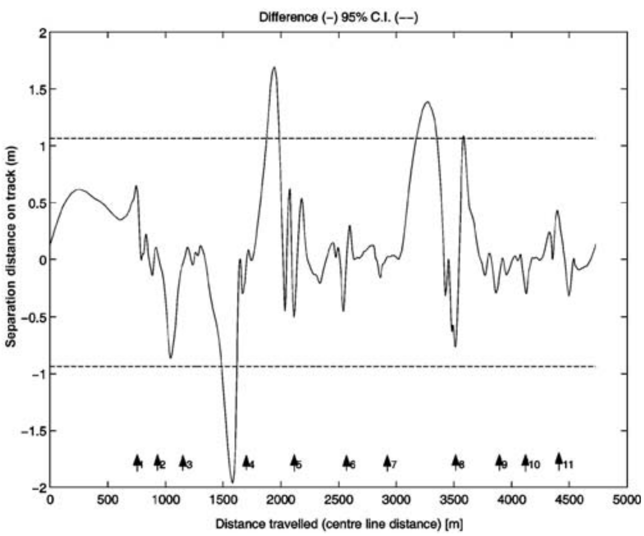

Fig. 10 Differences in the optimal line owing to a 6 per cent CG set-up change

The majority of the points are very similar, and this explains why the 95 per cent confidence interval is only ± 1.0 m. Drivers will struggle to follow the optimal path to ± 1.0 m at racing speed, so a knowledge of the change in optimal line may not be useful to them.

In section 4.1 it was found that an estimate of the average variability about the optimal line for the base set-up was ± 0.5 m at the 95 per cent confidence level. The differences between the CG optimal line and the base optimal line are ± 1.0 m at the 95 per cent confidence level. Both of these intervals are not particularly large considering the actual circuit width of 10 m, and the variability in the optimal line calculation represents half the observed difference between the base optimal and CG optimal lines. The interesting point will be the effect on the overall lap time of the CG car set-up and the racing line change. To make the comparison, the fastest lines from both the base and CG set-ups were used.

The lap times are calculated using the QSS method and are given in Table 3. The lap times, as found using the TO method [**17**], are also given for comparison. The agreement with the TO method lap

Table 3 Simulated lap time at the Barcelona Grand Prix circuit

Set-up	Lap time (s), QSS	Lap time (s), TO [**17**]
Base	82.904	80.714
CG change	81.471	80.177
Difference	1.433	0.537

times is good (within 3 per cent), and it appears that a positive set-up change has been made because the lap time has reduced in both cases.

To determine the reasons for this improvement it is necessary to inspect the acceleration time histories for the two set-ups (Fig. 11). The main differences in the accelerations between the two set-ups are the higher lateral acceleration peaks and the correspondingly higher (or lower if decelerating) longitudinal acceleration peaks in the CG optimal line results when compared with the base optimal line results. The CG vehicle on the CG line utilizes the improvements in lateral acceleration under tractive acceleration seen in Fig. 9 in corners 3, 7, and 11 (Fig. 11). The loss of lateral acceleration in braking appears to have very little impact. This is probably because the majority of braking is conducted in a straight line or close to it. As would be expected, this results in a better overall lap time for the CG optimal line (Table 3). The improvements in the three corners mentioned is confirmed in Fig. 12. This figure is a measure of the distance between the two cars as if they were racing each other. As can be seen, the CG vehicle creates gaps in corners 3, 7, and 11 that, by the end of the lap, results in a separation distance of 108 m which at the start/finish line speed of 76 m/s accounts for the 1.43 s lap time difference.

4.2.3 *Vehicle change or line change?*

The fact that the QSS method requires a line to be provided as an input can be exploited in a manner that is difficult with an optimization method that has

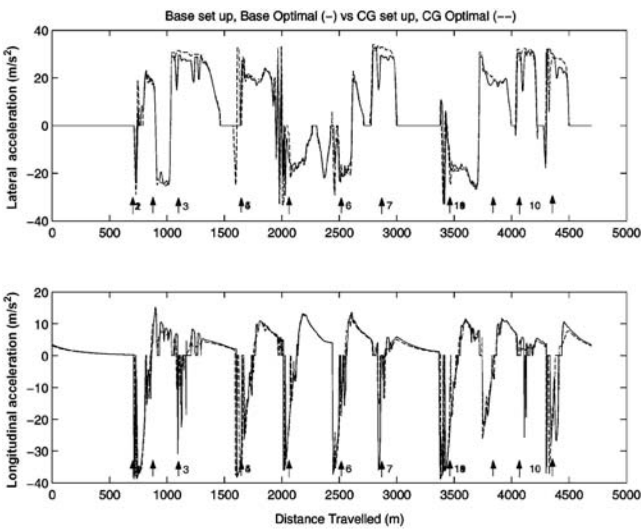

Fig. 11 Accelerations comparison – base set-up and CG set-up

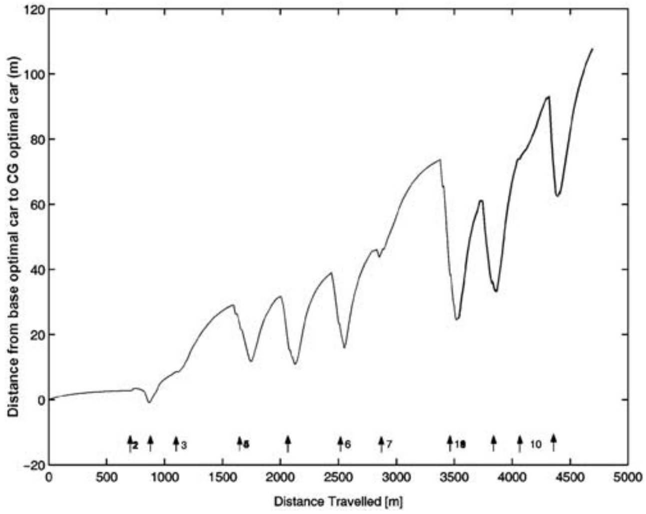

Fig. 12 Distance from the base optimal vehicle to the CG optimal vehicle

the racing line and control inputs coupled together as in reference [**17**]. The QSS method can run the CG vehicle behavioural characteristics which are stored as a vehicle-dependent, circuit-independent GG speed diagram with any choice of racing line. This allows the running of the CG vehicle with the base optimal line instead of the CG optimal line. This uncoupling allows the determination of the reason for the lap time improvement to be broken down into its potential causes, new optimal line and new vehicle, and analysed separately. Interestingly, the results show that the lap time of the CG vehicle on the base optimal line was virtually identical to that of the CG vehicle on the CG optimal line (Table 4).

A similar analysis of acceleration profiles and virtual car separation distances to that in section 4.2.2 will be used here to explain why this result occurred.

Figure 13 shows the acceleration histories for the CG vehicle using the base optimal and CG optimal racing lines. Unlike in Fig. 11, there are very few differences between the acceleration profiles. The differences are in corners 3, 7, and 11 again, but they are much smaller this time.

Table 4 Simulated lap time using the CG vehicle at the Barcelona Grand Prix circuit

Set-up	Lap time (s), QSS
Base optimal line	81.531
CG optimal line	81.471
Difference	0.06

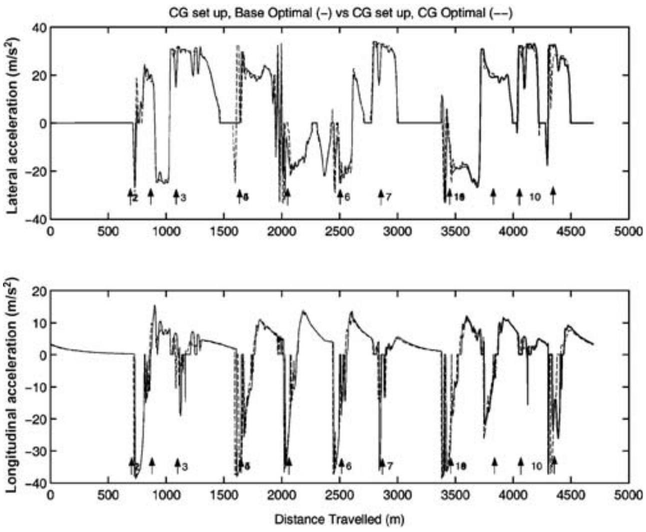

Fig. 13 Acceleration comparison – CG vehicle on base optimal and CG optimal racing lines

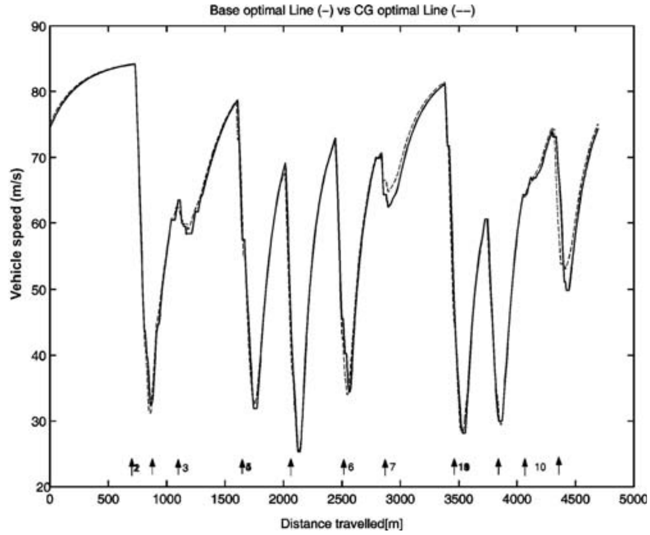

Fig. 15 Base optimal and CG optimal racing line speed history

Looking at the car separation distance plot in Fig. 14, it can be seen that the car separation distance never exceeds 8 m.

Figure 15 shows the speed history of the CG vehicle calculated for the base optimal and CG optimal racing lines. The speed profiles confirm that the differences are in corners 3, 7, and 11 and that they are relatively small. These corners are all high-speed corners ($\geqslant 50$ m/s), and inspection of Fig. 9 shows that in traction this is one of the areas where the GG speed diagram has expanded significantly. Looking back at Fig. 10 at these corners, it can be seen that they all vary by $\leqslant 0.5$ m from the base optimal line. This means that it is not possible to determine whether the small differences in lap time are due to exploitation of the new vehicle characteristics or variability in the optimal line calculation.

However, the results in Tables 3 and 4 suggest that moving the CG rearwards makes the car quicker around the circuit, as long as the path taken is very close to (but not necessarily exactly equal to) the optimal path. It would seem from this result that more attention should be placed on the track-independent handling characteristics of the car than on attempting to find a new optimal line for every set-up. The QSS method presented here is well suited to that approach. It would also seem that a method of producing faster lap times is to move the CG rearwards and then to find a driver who is able to get within half a metre of the notional optimal racing line, with a car that is now much harder to control on the limit.

The ability to separate the analysis of the vehicle set-up to that of the racing line is a useful feature of this QSS method. The analysis of the results has shown that the 6 per cent change in CG location towards the rear of the vehicle has produced a significant lap time improvement at the Barcelona Grand Prix circuit. The analysis of the racing line while using the CG vehicle has shown that very little of this improvement was due to the new optimal line. There is no reason to suspect that this is not a general result applicable to all open wheel race cars that have a long wheel base and a well-damped yaw response.

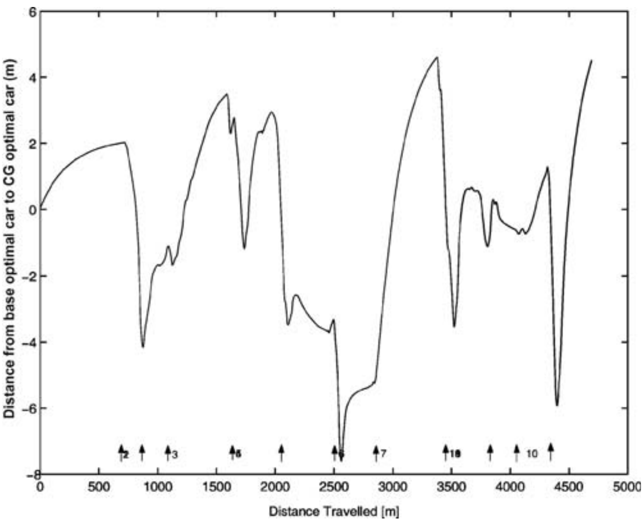

Fig. 14 Distance from the base optimal CG vehicle to the CG optimal CG vehicle

5 PRACTICAL RACING LINE EXPERIMENT

The research presented so far has been based purely on numerical modelling and analysis. As an interesting exercise that supplements the racing line argument, a small group of four experienced racing drivers were provided with a two-corner section of the Barcelona Grand Prix circuit and asked to draw their preferred racing line with a permanent marker. The drivers were interviewed separately.

The marked lines were then digitized on a PC and thinner digital lines were constructed from the averages of the marked lines. This made the comparison easier to make through the use of different line styles, and the reduction in line thickness created a small allowance for the vehicle track width which was deemed more realistic. The result is shown in Fig. 16.

The four drivers are current professional racing drivers, and all the racing lines are based on a line taken with a similar type of open wheel race car. This experiment, while interesting, suffered some obvious shortcomings in the method, with the most obvious one being that drawing the line as accurately as the driver intended was difficult. However, if one uses the result to look at driving trends, then useful qualitative information can be extracted from the experiment.

The differences in the lines taken by the four drivers are more than ± 1 m, which adds further weight to the conclusion that a change in racing line of ± 1 m may be of limited practical value to a racing driver. Three of the four drivers suggest a very late turn into the first corner, to allow for a very tight exit of the corner, with the aim of improving exit speed. Driver 1 chose an earlier turn into corner 1 and to sacrifice hitting the corner apex and following a wider mid-corner and corner exit trajectory. Driver 1, who took the earlier corner entry trajectory, suggested that the line taken in a traction-controlled vehicle would depend very much on the behaviour of the traction control system. If the traction control system cut in relatively early, driver 1 would adopt a wider trajectory through corner 1 to help improve the traction and therefore speed through the corner.

Through corner 2, three of the drivers appear to converge on the same trajectory, with corner entry started out at the edge of the circuit, before turning in as close as possible to the apex of the corner, and then reducing the steer angle to control the vehicle towards the outside of the track on corner exit. Again, one driver, this time driver 2, took a later turn into corner 2, although the same mid-corner and corner exit trajectory was suggested as the other three drivers. The severity of the change in trajectory towards the apex of corner 2 of driver 2's trajectory suggests that this was likely to be a drawing error, and if redrawn would more closely approximate the other three driver trajectories.

This analysis of the racing lines shown in Fig. 16 indicates that there is more to the process of driving the racing line than just putting the car on the limit at all times, as the optimal path finding methods do. Other relevant factors include: low road friction conditions off the most frequently used racing line, the effect of active systems, and driver prejudice.

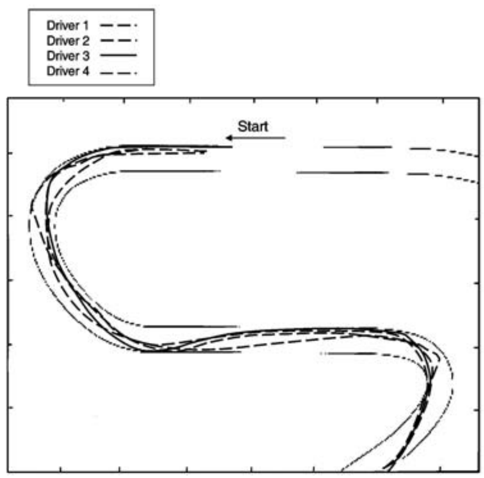

Fig. 16 Racing line experiment – British F3 drivers

6 CONCLUSIONS

The quasi steady state method described here is a good approximation to the optimized transient solution for a 7DOF vehicle model. The computation time has been significantly reduced from hours to minutes, with little significant effect on the results obtained.

The quasi steady state method and the transient optimal method both show improvements in lap time owing to a 6 per cent centre of gravity set-up change, and the quasi steady state method produces a lap time that is within 3 per cent of the transient optimal method result.

The difference in optimal lines caused by a 6 per cent CG change is shown to be so small that the driver is unlikely to find the information useful. In light of this observation, the computational effort required to generate a new optimal line for each set-up change may be misspent.

REFERENCES

1 **Siegler, B., Deakin, A.,** and **Crolla, D.** Lap time simulation: Comparison of steady state, quasi-static and transient racing car cornering strategies. In Proceedings of 2000 SAE Motorsports Engineering Conference and Exposition, 2000, SAE paper 2000-01-3563 (Society of Automotive Engineers, Warrendale, Pennsylvania).

2 **Candelpergher, A., Gadola, M.,** and **Vetturi, D.** Developments of a method for lap time simulation. In Proceedings of 2000 SAE Motorsports Engineering Conference and Exposition, 2000, SAE paper 2000-01-3562 (Society of Automotive Engineers, Warrendale, Pennsylvania).

3 **Blasco-Figueroa, J.** Minimum time manoeuvre based on the GG-speed envelope. Master's thesis, School of Engineering, Cranfield University, 2000.

4 **Muehlmeier, M.** and **Mueller, N.** Optimization of the driving line on a race track. In Proceedings of 2002 SAE Motorsports Engineering Conference and Exposition, 2002, SAE paper 2002-01-3339 (Society of Automotive Engineers, Warrendale, Pennsylvania).

5 **Butz, T., Ehmann, M., von Stryk, O.,** and **Wolter, T.** Realistic road modelling for the real-time simulation of vehicle dynamics. *Automobiltech. Z.*, February 2004, **106**, 118–125.

6 **Milliken, W.** and **Milliken, D.** *Race Car Vehicle Dynamics*, 1995 (Society of Automotive Engineers, Warrendale, Pennsylvania).

7 **Wright, P.** *Formula 1 Technology*, 2001 (Society of Automotive Engineers, Warrendale, Pennsylvania).

8 **Casanova, D.** On minimum time vehicle manoeuvring: the theoretical optimal lap. PhD thesis, School of Engineering, Cranfield University, 2000.

9 **Sharp, R.** The application of multi-body computer codes to road vehicle dynamics modelling problems. *Proc. Instn Mech. Engrs, Part D: J. Automobile Engineering*, 1995, **208**, 55–61.

10 **Fujioka, T.** and **Kimura, T.** Numerical simulation of minimum-time cornering behaviour. *JSAE Rev.*, 1992, **13**(1), 44–51.

11 **La Joie, J.** Race car performance optimization. Technical report SAE 942492, Society of Automotive Engineers, 1994.

12 **Hendrikx, J., Meijlink, T.,** and **Kriens, R.** Application of optimal control theory to inverse simulation of car handling. *Veh. Syst. Dynamics*, 1996, **26**, 449–462.

13 **Allen, J.** Computer optimisation of cornering line. Master's thesis, School of Engineering, Cranfield University, 1997.

14 **Walsh, G.** *Methods of Optimization*, 1977 (John Wiley).

15 **Pacejka, H.** and **Besselink, I.** Magic formula tyre model with transient properties. *Veh. Syst. Dynamics Suppl.*, 1997, **27**, 234–249.

16 **Casanova, D., Sharp, R.,** and **Symonds, P.** On minimum time optimisation of formula one cars: the influence of vehicle mass. In Proceedings of AVEC'2000, International Symposium on *Advanced Vehicle Control*, Ann Arbor, Michigan, 2000.

17 **Casanova, D., Sharp, R.,** and **Symonds, P.** On the optimisation of the longitudinal location of the mass centre of a formula one car for two circuits. In Proceedings of AVEC'2002, International Symposium on *Advanced Vehicle Control*, Hiroshima, Japan.

18 **Casanova, D., Sharp, R.,** and **Symonds, P.** Minimum time manoeuvring: the significance of yaw inertia. *Veh. Syst. Dynamics*, 2000, **34**(2), 77–115.

19 **Griffiths, R.** Minimum lap time simulation of a racing car. Master's thesis, School of Mechanical Engineering, Cranfield University, September 1992.

20 **Murdoch, A.** 'GG' speed surface approach to minimum lap time simulation. Master's thesis, School of Mechanical Engineering, Cranfield University, September 2001.

21 **Coleman, T., Branch, M.,** and **Grace, A.** Matlab optimisation toolbox version 2 user guide. Technical report, MathWorks, Natick, Massachusetts, 1999.

22 **How, J., Pohlman, N.,** and **Park, C.-W.** GPS estimation algorithms for precise velocity, slip and race-track position measurements. In Proceedings of 2000 SAE Motorsports Engineering Conference and Exposition, 2000, SAE paper 2002-01-3336 (Society of Automotive Engineers, Warrendale, Pennsylvania).

23 **Siegler, B.** and **Crolla, D.** Lap time simulation for racing car design. In Proceedings of SAE 2002 World Congress and Exhibition, 2002, SAE paper 2002-01-0567 (Society of Automotive Engineers, Warrendale, Pennsylvania).

24 **Jang, J.-H.** and **Han, C.-S.** The sensitivity analysis of lateral acceleration for the front wheel steering vehicle in the frequency domain. *Int. J. Veh. Des.*, 1998, **19**(4), 415–435.

25 **Crolla, D.** An introduction to vehicle dynamics. Vehicle Dynamics Group, Department of Mechanical Engineering, University of Leeds, UK, 1991.

APPENDIX

Notation

a_y	steady state lateral acceleration (m/s^2)
f	objective function
$\mathbf{G}$	constraint matrix
$\boldsymbol{P}$	optimization vector
r	corner radius (m)
s	distance (m)
T_p	throttle position
x	position of the centre of gravity of the vehicle in the longitudinal direction (m)
$\dot{x}$	vehicle speed (m/s)
$\ddot{x}$	longitudinal acceleration (m/s^2)
y	position of the centre of gravity of the vehicle in the lateral direction (m)
$\dot{y}$	lateral speed (y axis) (m/s)
$\ddot{y}$	lateral acceleration (y axis) (m/s^2)

δ steer angle (rad)
$\dot{\theta}_{F}$ front wheel angular speed (rad/s)
$\dot{\theta}_{LF}$ left front wheel angular speed (rad/s)
$\ddot{\theta}_{LF}$ left front wheel angular acceleration (rad/s^2)
$\dot{\theta}_{LR}$ left rear wheel angular speed (rad/s)
$\ddot{\theta}_{LR}$ left rear wheel angular acceleration (rad/s^2)
$\dot{\theta}_{R}$ rear wheel angular speed (rad/s)
$\dot{\theta}_{RF}$ right front wheel angular speed (rad/s)
$\ddot{\theta}_{RF}$ right front wheel angular acceleration (rad/s^2)
$\dot{\theta}_{RR}$ right rear wheel angular speed (rad/s)
$\ddot{\theta}_{RR}$ right rear wheel angular acceleration (rad/s^2)
$\dot{\varphi}$ yaw rate (rad/s)
$\ddot{\varphi}$ yaw acceleration (rad/s^2)